JOURNAL OF CATALYSIS 157, 450–460 (1995)

Electrocatalytic Synthesis of Propylene Oxide during Water Electrolysis

Kiyoshi Otsuka, Tetsuya Ushiyama, Ichiro Yamanaka, and Kohki Ebitani

Department of Chemical Engineering, Tokyo Institute of Technology, Ookayama, Meguro-ku, Tokyo 152, Japan

Received April 21, 1995; revised July 5, 1995; accepted July 26, 1995

A new method for the synthesis of propylene oxide using nascent oxygen generated during the electrolysis of water has been proposed. Among the noble metal blacks tested, the most active and selective anode electrocatalyst was Pt black. The oxidation of propylene was initiated at an applied voltage across the cell higher than ca. 1.1 V (anode potential higher than 1.1 V vs NHE). The formations of propylene oxide and acetone were enhanced remarkably at >1.1 V applied voltage. The maximum oxidation efficiency for the sum of the two products was 56% at an applied voltage of 1.5 V (anode potential 1.3 V vs NHE). The epoxidation at applied voltage higher than 1.5 V enhanced the formation of by-products, CO_2 > acetic acid ≥ propionic acid. The kinetic curves of each product suggest that propylene oxide and acetone are formed in parallel; neither acetone, nor CO_2, nor acetic acid are formed from the propylene oxide produced. The method was more effective for epoxidations of 1-hexene and *cis*- and *trans*-2-hexenes. The product ratio in *cis*- and *trans*-2,3-epoxyhexanes observed for the epoxidations of the 2-hexenes indicated the retention of the *cis–trans* configuration of the starting 2-hexenes. The oxidations of cyclohexane and benzene by the same method were quite slow, giving CO_2 as the main product. Thus, the active oxygen generated in this system was quite specific for epoxidation of olefins. The calcination of an inactive Pt black in air at ca. 673 K enhanced remarkably its electrocatalytic activity for epoxidation of olefins. XPS studies on various Pt black samples suggested that the PtO_2 phase was responsible for the formation of the active oxygen. A tentative Langmuir–Hinshelwood-type reaction mechanism has been proposed to account for the epoxidation results. © 1995 Academic Press, Inc.

INTRODUCTION

Propylene oxide is one of the most useful synthetic intermediates in the current chemical industry. Propylene oxide is produced either by the chlorohydrin or the hydroperoxide process (1). These commercial processes are made up of indirect, multistep operations for the synthesis of propylene oxide with stoichiometric coproduction of various byproducts. Moreover, these processes use an environmentally hazardous compound, chlorine, or labile explosive and expensive oxidants, hydroperoxides. Therefore, a simple and environmentally gentle one-step synthesis of propylene oxide is keenly desired. Direct epoxidation of olefins by hydrogen peroxide has been a long-standing goal in this respect (2–5). However, the influence of H_2O_2 cost and availability is a limitation for industrial exploitation. The attempt to design catalytic systems that would directly oxidize olefins to epoxides using oxygen and a coreductant, hydrogen (6–9), is attractive but a careful handling is stringently required for the explosive oxygen–hydrogen gas mixture. Although one may use other reductants such as $NaBH_4$ (10), sodium ascorbate (11), Zn/CH_3COOH (12, 13), and various aldehydes (14–16), these reductants are much more expensive than hydrogen and the catalytic systems are rather complicated.

Electrolysis of water with an acid electrolyte (H_2SO_4, H_3PO_4, polyfluorocarbon sulfonic acid) produces oxygen and hydrogen at the anode and the cathode, respectively, according to the electrochemical reactions

(Anode)

$$2H_2O \rightarrow O_2 + 4H^+ + 4e^- \quad [1]$$

(Cathode)

$$2H^+ + 2e^- \rightarrow H_2. \quad [2]$$

We can expect that the hydrogen-stripped atomic oxygen atoms (O*) from water at the anode, before their recombination into an oxygen molecule or the nascent diatomic oxygen species (O_2*) just after their formation, might have a very special reactivity toward olefins in the presence of a specific anode electrocatalyst. In fact, we have demonstrated the epoxidation of cyclohexene by means of a nascent oxygen generated on a Pd-anode during the electrolysis of water (17). However, the current efficiency for the synthesis of epoxide was quite low (<4.5%). Moreover, the epoxidation of propylene on this electrocatalyst was not successful.

In this report we describe our finding that the active

0021-9517/95 $12.00

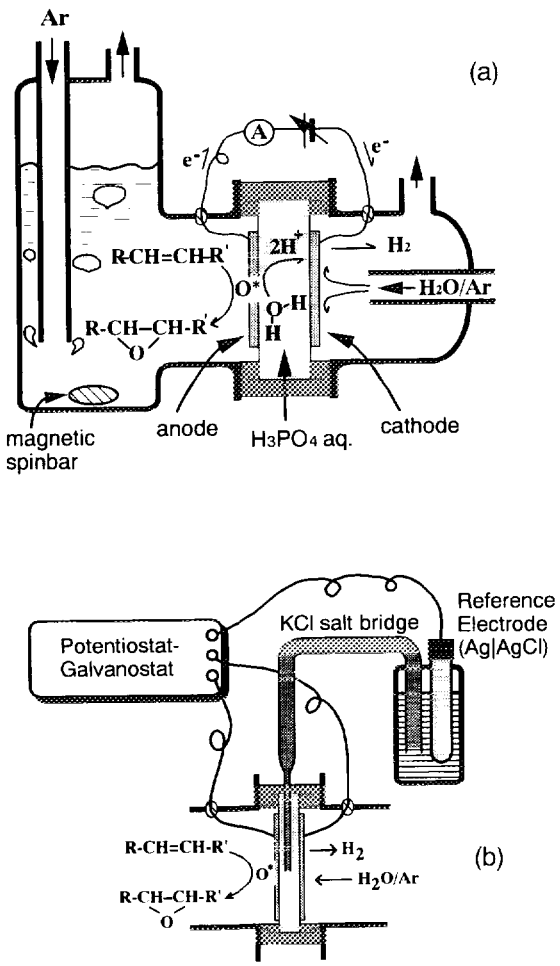

FIG. 1. (a) Schematic diagram of the reactor and the principle of the method for epoxidation of olefins during electrolysis of water. (b) Instrumental arrangement for the potential measurement.

oxygen generated on a Pt-black anode epoxidizes propylene and 1-hexene with a fairly high selectivity and current efficiency. The nature of the active oxygen and the reaction mechanism of the epoxidation will be discussed.

EXPERIMENTAL

The electrocatalysts used were all reagent grade noble metal blacks (purity >99%) obtained from Wako Pure Chemical Company, Kanto Kagaku Industry, and Soekawa Rikagaku Industry. The Pt black we prepared by reduction of H_2PtCl_6 with $NaBH_4$ in ethanol was also tested.

The propylene used was an extra-pure gas (>99.95%) purchased from Takachiho Chemical Company. 1-Hexene and 2-hexene were purified by distillation before use.

The reactor and the principle of the method for the epoxidations of propylene and 1-hexene mediated by electrolysis of water are shown schematically in Fig. 1a. A silica-wool disk (21 mm diameter, 2 mm thickness) containing aqueous H_3PO_4 separates the anode and the cathode compartments. Propylene was bubbled into the CH_2Cl_2 (40 cm^3 used as a solvent) at the anode compartment. In the case of 1-hexene oxidation, 10 cm^3 of the olefine was dissolved in 30 cm^3 of CH_2Cl_2, and argon was bubbled into the anode compartment to remove the oxygen evolved during the reaction. The anode electrocatalysts were prepared from the Pt black or other metal blacks (70 mg) mixed with Teflon powder (1 mg as a binder) by the hot-press method. The mixture was pressed and shaped into a round wafer (20 mm diameter, 0.1 mm thickness) on a hot plate (393 K). The cathode was prepared in the same way from the mixture of Pt black (Wako 20 mg), graphite (50 mg), and Teflon powder (5 mg). Argon (98 kPa) and water vapor (4 kPa) were passed through the cathode compartment to prevent the electrolyte from dryness as well as to remove hydrogen during the electrolysis. The oxidation of olefins was initiated by applying a voltage between both electrodes.

The experiments for oxidations of propylene and 1-hexene were performed under the following conditions unless otherwise stated: reaction temperature, 303 K; flow rate of propylene or argon, 5 cm^3 STP; pressure of propylene or argon, 101 kPa; H_3PO_4 aq. 1 *M*, 0.65 g; applied voltage, 1.70 V; reaction time, 120 min. The total gas pressure for both cathode and anode sides was 101 kPa. The current and the applied voltage across the cell were monitored with a multimeter (Yokokawa 2506A). The anode and the cathode potentials during reaction under applied voltage were measured with reference to a Ag/AgCl reference electrode by using a potentiostat–galvanostat (Hokuto HA-301) with a KCl salt-bridge connected to the electrolyte (H_3PO_4) in a silica-wool disk as demonstrated in Fig. 1b and elsewhere (18). The potentials measured were corrected to the values vs NHE by adding 0.196 V.

The products were analyzed by gas-chromatography with 1-butanol or 1-adamantanol as an internal standard using columns PEG-20M, Sorbitol, and Gaskuropack 54.

The reproducibility in the preparation of the anode was examined on the basis of that in the amounts of products under the same reaction conditions. Carefully prepared electrodes guaranteed a reproducibility of ±10%.

The oxidation efficiency (OE) for the formation of the oxygenate concerned was defined as

$$\mathrm{OE} = \frac{\text{amount of the oxygenate formed (mol)}}{\text{amount of oxygen atoms produced during water electrolysis (mol)}} \times 100\%,$$

where the denominator was calculated from the charge passed during the reaction.

The XPS measurement of different Pt black samples was

made using a VG ESCALAB 220-1 spectrometer with Mg Kα X-rays (1253.6 eV) under vacuum conditions better than 1.0×10^{-7} kPa. In a typical XPS measurement, 30 spectra were accumulated (step width, 0.1 eV; pass energy, 20 eV). The binding energy was calibrated with reference to the value of Pt 4*f* of Pt metal (71.2 eV) (19–21). The separation of Pt 4*f* XPS peaks into platinum metal (Pt^0) and cation (Pt^{4+}) was performed using a theoretical intensity ratio of Pt $4f_{7/2}$ to Pt $4f_{5/2}$ equal to 4/3 and a peak separation of 3.3–3.4 eV (19–21). The background subtraction was performed using Shirley's method (22). The peaks were separated by using a Gaussian/Lorentzian product function (23).

RESULTS AND DISCUSSION

Preliminary experiments indicated that a Pt black obtained from Wako Pure Chemical was the most active electrocatalyst among the noble metals tested (Pd, Pt, Rh, Ru, Au) for epoxidation of 1-hexene into 1,2-epoxyhexane during water electrolysis (24). However, some Pt blacks obtained from different makers (Kanto Kagaku, Soekawa) showed only a weak catalytic activity for the epoxidation of 1-hexene. The Pt black we prepared from H_2PtCl_6 by reduction with $NaBH_4$ in ethanol did not give a high catalytic activity either. However, after a pretreatment in air at 673 K, all the Pt blacks examined in this work showed a fairly good current efficiency for the formation of 1,2-epoxyhexane. These observations suggest that the formation of Pt oxides at least at the surface of Pt black particles are responsible for the epoxidation. The XPS study on this point will be described in detail later.

The oxidation pretreatment in air for the other noble metal blacks (Pd, Rh, Ru, and Au) did not generate a catalytic activity for the synthesis of epoxides. The electrocatalytic activity of the Pt black obtained from Wako was not influenced by the calcination pretreatment in air at 673 K. The catalytic activity of this material was stable and slightly higher than those of the other Pt blacks which had been activated by calcination in air. Therefore, most of the study in this work has been performed with this Pt black (Wako) electrocatalyst unless otherwise stated.

I. Epoxidation of Propylene

Effect of applied voltage. The reaction of propylene under the standard experimental conditions gave propylene oxide and acetone as the main products and a trace of propionic acid, acetic acid, and CO_2. The changes in the amounts of products as functions of the applied voltage across the cell are shown in Fig. 2. The applied voltage here means the applied anode potential with reference to the cathode. The charge passed (C.P.) and the oxidation efficiency for the formation of propylene oxide and for the sum of propylene oxide and acetone are also plotted in

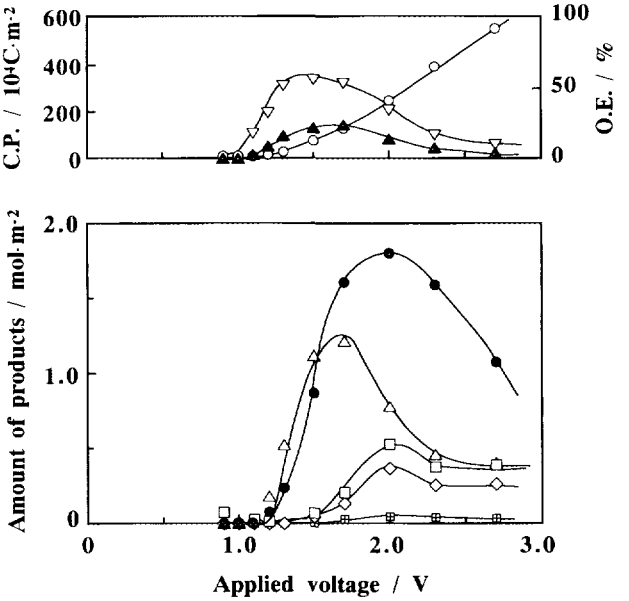

FIG. 2. Partial oxidation of propylene as a function of applied voltage. Standard reaction conditions: T = 303 K, reaction time = 2 h, concentration of H_3PO_4 = 1.0 mol·dm^{-3}. Anode, Pt black, $P(C_3H_6)$ = 101 kPa. Cathode, Pt black/graphite, $P(H_2O)$ = 3 kPa, $P(Ar)$ = 98 kPa. Flow rate = 5 ml·min^{-1} (anode), 10 ml·min^{-1} (cathode). Propylene oxide (●); acetone (△); propionic acid (☒); acetic acid (◇); CO_2 (□); charge passed (○); oxidation efficiency for the sum of propylene oxide and acetone (▽); oxidation efficiency of propylene oxide (▲).

Fig. 2. The results in Fig. 2 show that the oxidation of propylene is initiated at an applied voltage greater than 1.1 V. It should be noted that the oxidation occurs at a voltage lower than 1.23 V, the thermodynamically required voltage for the electrolysis of water.

Compared to the increase in the charge passed, the amount of acetone and propylene oxide increased remarkably with a rise in the voltage at 1.1 ~ 1.7 V. Thus, the oxidation efficiencies for propylene oxide and for the sum of oxygenates are also improved considerably. The maximum oxidation efficiency for the sum of propylene oxide and acetone was 56% at 1.50 V. This is a remarkably high oxidation efficiency compared to that obtained in the oxidation of cyclohexene using Pd black as an electrocatalyst (17). The increase in the applied voltage above 1.6 V decreased the rate of acetone formation sharply. The decrease in the formation rate was also observed for propylene oxide at >1.9 V. Therefore, the oxidation efficiencies dropped sharply at >1.7 V. The formation of acetic acid and CO_2 increased at >1.5 V; thus they are no longer minor products at higher applied voltages.

Effects of propylene pressure and reaction temperature. The rate of formation of propylene oxide under a constant applied voltage of 1.7 V increased with a rise in the partial pressure of propylene bubbled into the solvent

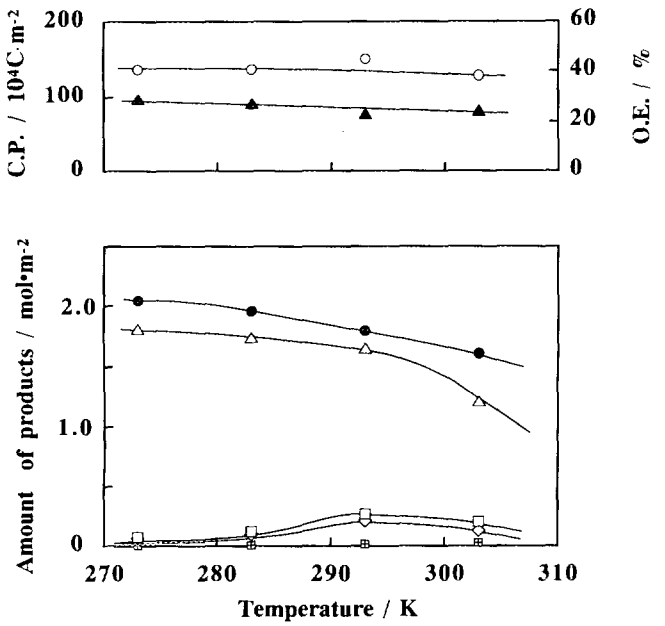

FIG. 3. Effect of reaction temperature on epoxidation of propylene. Standard reaction conditions. Propylene oxide (●); acetone (△); propionic acid (☒); acetic acid (◇); CO_2 (□); charge passed (○); oxidation efficiency of propylene oxide (▲).

(CH_2Cl_2). The current or the charge passed at 1.7 V, however, did not change with the pressure of propylene. The formation rates of the by-products (CO_2, acetic acid, and propionic acid) were not enhanced with increased pressure of propylene. Thus, the oxidation efficiency for propylene oxide was improved considerably with propylene pressure.

Figure 3 shows the effects of reaction temperature on the amount of each product formed in 2 h, on the oxidation efficiency for the formation of propylene oxide and on the charge passed. The formation rates of propylene oxide and acetone are improved by decreasing the reaction temperature. On the contrary, the formations of CO_2 and acetic acid were depressed. The current or the charge passed did not change with temperature. Thus, the oxidation efficiency for the synthesis of the epoxide was improved to 30% at the lowest temperature (273 K) tested in this work.

Effect of the concentration of H_3PO_4. The concentration of H_3PO_4 (aq.) in the silica-wool disk affected the oxidation of propylene dramatically, as can be seen in Fig. 4. The oxidation efficiency for the sum of propylene oxide and acetone becomes 60% at a H_3PO_4 concentration of 0.5 mol · dm^{-3}. However, the maximum oxidation efficiency for the propylene oxide is obtained at a concentration of 1.0 mol · dm^{-3}. The sharp drop in the formation rates of both propylene oxide and acetone at >1.0 mol · dm^{-3} and at <0.5 mol · dm^{-3} can be ascribed to the decrease in the current or the charge passed due to the increase in the ohmic resistance of the electrolyte at these concentration regions.

Oxidation in the presence of O_2 at the cathode. The same experiments as those in Fig. 2 have been performed by changing the gas in the cathode compartment from helium to oxygen (98 kPa). This replacement of the cathode gas reduced the applied voltage needed for the initiation of the oxidation of propylene by about 0.5 V, i.e., the formation of propylene oxide and acetone occurred at an applied voltage >0.6 V. The curves for the amount of products and the current as functions of the applied voltage obtained for the cell with oxygen at the cathode would be superimposed on those in Fig. 2 if the applied voltage for the former were subtracted by ca. 0.5 V. This indicates that the replacement of helium in the cathode compartment by oxygen decreases the applied voltage required for obtaining the same rate of formation of each product and the current. Under these circumstances, the presence of oxygen (or air) in the cathode compartment saves the electric energy required for the synthesis of propylene oxide. The reduction of the applied voltage by ca. 0.5 V can be ascribed to the overpotential difference between hydrogen evolution (in the case of He) and oxygen reduction (in the presence of O_2) at the cathode.

Kinetic curves of each product. The reaction paths for the formation of by-products (acetone, acetic acid, CO_2,

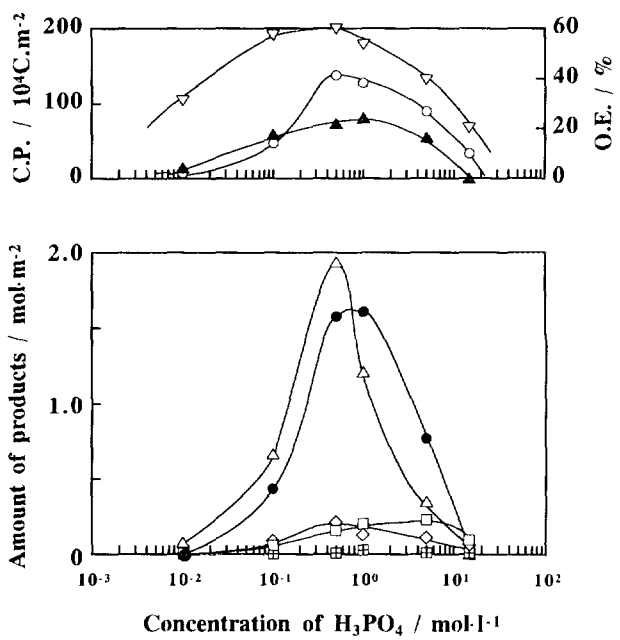

FIG. 4. Effect of the concentration of H_3PO_4 on oxidation of propylene. Standard conditions. Propylene oxide (●); acetone (△); propionic acid (☒); acetic acid (◇); CO_2 (□); charge passed (○); oxidation efficiency for the sum of propylene oxide and acetone (▽); oxidation efficiency of propylene oxide (▲).

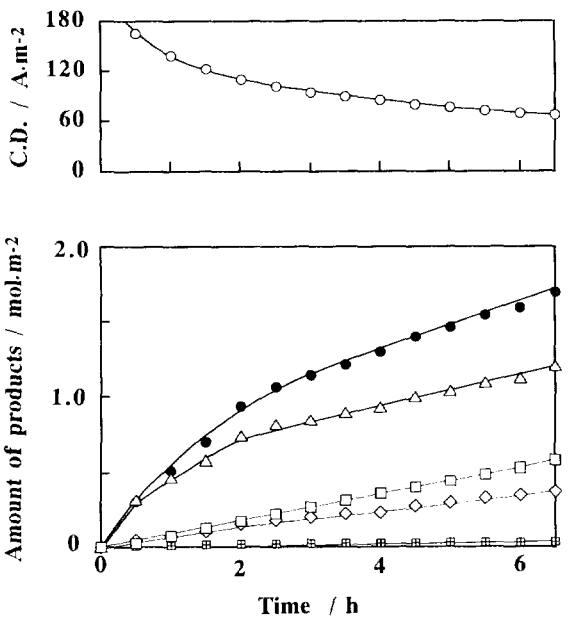

FIG. 5. Kinetic curves for the products in oxidation of propylene. Standard conditions. Propylene oxide (●); acetone (△); propionic acid (⊠); acetic acid (◇); CO_2 (□); current density (○).

and propionic acid) may be suggested by observing the kinetic curves for each product. Therefore, the kinetic curves obtained under the standard reaction conditions are shown in Fig. 5. The amount of each product accumulated and the current density are plotted as functions of the reaction time. The parallel kinetic curves of propylene oxide and acetone in Fig. 5 suggest that the two products are formed concurrently, probably from a common reaction intermediate. It should be noted that the formation rates of acetic acid and CO_2 are not accelerated with accumulation of propylene oxide or acetone. This suggests that the acetic acid and CO_2 are produced neither from propylene oxide nor from acetone by their further oxidation. The addition of propylene oxide to the starting substrate in CH_2Cl_2 with an amount comparable to that obtained in 2 h under standard reaction conditions neither retarded nor accelerated the rates of formations of acetone, CO_2, acetic acid, and propionic acid. In other words, the kinetic curves of the formations of these by-products were identical to those obtained without the addition of propylene oxide. These facts strongly suggest that neither acetone, CO_2, nor acetic acid are formed from the propylene oxide produced. The reaction path for propionic acid cannot be discussed because of its trace amount.

Effect of O_2, H_2O_2, and tert-BuOOH. The total oxidation efficiency for the sum of the oxidation products was ca. 60% at the highest. This means that most of the oxygen discharged at the anode evolves into the gas phase as O_2. The gaseous oxygen bubbled into the anode compartment under standard reaction conditions, however, did not affect the oxidation of propylene at all, i.e., the reaction was neither accelerated nor retarded in the presence of gaseous oxygen in the anode compartment.

The effects of the addition of H_2O_2 and *tert*-butylhydroperoxide (*tert*-BuOOH) to a CH_2Cl_2 solvent were examined under the standard reaction conditions. The amount of each oxidant was roughly adjusted to that of the water electrolyzed in 2 h under standard reaction conditions. H_2O_2 and *tert*-BuOOH did not initiate the oxidation of propylene under open-circuit conditions. Both oxidants rather retarded the oxidation under applied voltage. These observations may suggest that H_2O_2 and hydroperoxide cannot be the active oxygen species for the epoxidation of propylene in this work.

II. Oxidation of Various Other Hydrocarbons

Studies on the oxidations of other olefins, alkanes, and aromatics with the oxygen generated during water electrolysis may give us valuable information about the nature of the active oxygen species and the reaction mechanism of the epoxidation of propylene. Thus, we studied the oxidation of 1-hexene, 2-hexene, cyclohexane, and benzene under reaction conditions similar to those applied for the propylene oxidation.

a. 1-Hexene. The main products from 1-hexene oxidation were 1,2-epoxyhexane and 2-hexanone. The minor products were hexanoic acid > pentanoic acid > 1-hexanol and a trace of CO_2. The selectivity to the sum of the two main products was always greater than 90% under the reaction conditions used in this work.

The results of 1-hexene oxidation are shown in Fig. 6. The amount of products, the charge passed (C.P.), and the oxidation efficiencies (O.E.) for 1,2-epoxyhexane and for the sum of 1,2-epoxyhexane and 2-hexanone are plotted as functions of the applied voltage. The square symbols in this figure indicate the total amount of the minor products obtained in 2 h. Similar to the results of propylene oxidation (Fig. 2), the oxidation of 1-hexene is initiated at an applied voltage greater than ca. 1.1 V. The rates of formation of epoxide and 2-hexanone increase sharply with applied voltage and reach their maxima at ca. 2.5 V. The selectivity to 1,2-epoxyhexane was improved to 65% at an applied voltage >3.0 V. The maximum oxidation efficiencies to 1,2-epoxyhexane and to the sum of the epoxide and 2-hexanone are 35 and 68%, respectively, at 1.70 V. In general, the oxidation efficiency for 1-hexene oxidation (Fig. 6) is higher than that for propylene oxidation (Fig. 2).

The effects of concentration of H_3PO_4 on the rate of formation of products and on the oxidation efficiency and the charge passed have been examined at an applied voltage of 1.7 V over the concentration rate of 0.01 to 14.7

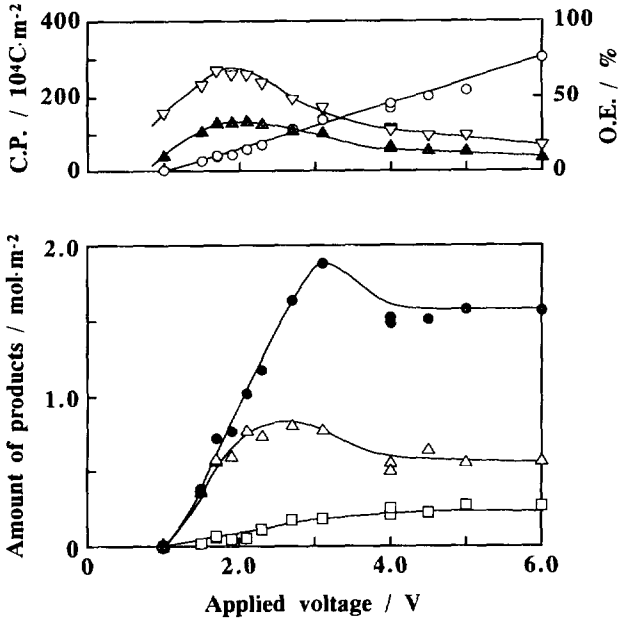

FIG. 6. Partial oxidation of 1-hexene as functions of applied voltage. Standard conditions. 1,2-Epoxyhexane (●); 2-hexanone (△); sum of minor products (□); charge passed (○); oxidation efficiency for the sum of epoxide and 2-hexanone (▽); oxidation efficiency of epoxyhexane (▲).

mol · dm^{-3}. The results were similar to those of Fig. 4, viz., the charge passed in 2 h showed a maximum at a concentration of 1 mol · dm^{-3}. However, the optimum H_3PO_4 concentration for the formation of both 1,2-epoxyhexane and 2-hexanone was ca. 0.2 mol · dm^{-3}. The maximum oxidation efficiencies for these products were obtained at 0.1 mol · dm^{-3}. Therefore, the concentration of H_3PO_4 for the experiments in Fig. 6 had been fixed at 0.1 mol · dm^{-3}.

b. cis- and trans-2-Hexenes. Oxidations of *cis*- and *trans*-2-hexenes were performed under standard reaction conditions. The main product was 2,3-epoxyhexane for both 2-hexenes. By-products were 2-hexanone and 2-hexanol with an amount less than 0.03 mol · m^{-2}. The yields of *cis*- and *trans*-2,3-epoxyhexanes obtained are listed in Table 1. It is to be noted that the *cis* or *trans* configuration of the substrate has been completely retained for the hexane oxides produced. This observation suggests that the rotation around the C(2)-C(3) axis of the activated complex, the oxygen-added 2-hexenes, is strictly prohibited. In other words, the activated complex cannot be a radical-type species which allows free rotation around the C(2)–C(3) axis. Both carbons at the 2- and 3-positions of the complex must be bonding, one to the oxygen and the other to the surface atoms. Moreover, the results in Table 1 indicate that the reactivity of the *cis* isomer is roughly twice as great as that of the *trans* isomomer, suggesting steric hindrance affects the formation of the precursor complex of the epoxides.

c. Cyclohexane and benzene. Oxidation of cyclohexane and benzene were examined under standard reaction conditions by replacing 1-hexene with cyclohexane or benzene. In the case of cyclohexane oxidation, although the charge passed in 2 h under an applied voltage of 1.7 V (90×10^4 C · m^{-2}) was comparable to that observed in 1-hexene oxidation (75×10^4 C · m^{-2}), the oxidation rate of cyclohexane was quite slow, i.e., the amounts of products were 0.02 and 0.03 mol · m^{-2} for cyclohexanone and CO_2, respectively. In the case of benzene oxidation, no oxygenated product was obtained. CO_2 was the only product with an amount of 0.25 mol · m^{-2} in 2 h.

Comparison of the results between olefins and those of cyclohexane and benzene described above indicates that the active oxygen generated on Pt black is quite specific for the epoxidation of olefins (propylene, 1-hexene, 2-hexenes).

d. Effect of calcination treatment of Pt black. As described earlier, the electrocatalytic activity of Pt black for epoxidation of 1-hexene depended on the formation of Pt oxides at the surface of Pt black. In this section, we describe more about the effect of the oxidation pretreatment of Pt black on the catalytic efficiency for the epoxidation.

Table 2 shows the effects of calcination pretreatment of

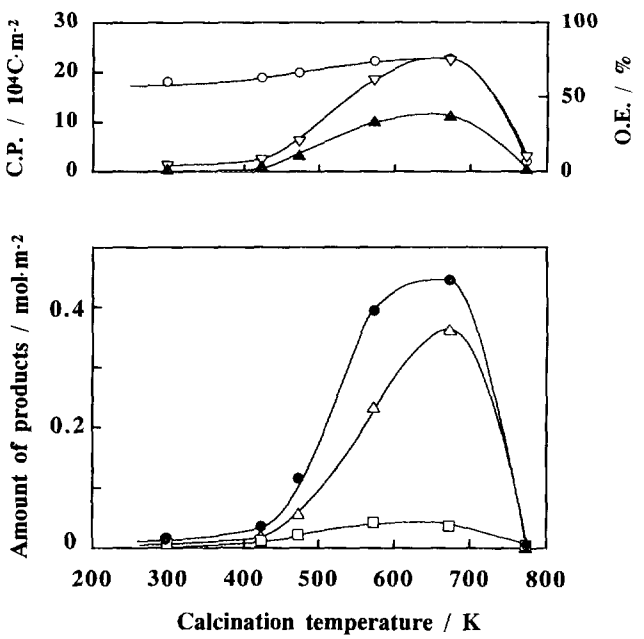

FIG. 7. Effect of calcination temperature for Pt-black anode (Kanto) on oxidation of 1-hexene. Standard conditions. 1,2-Epoxyhexane (●); 2-hexanone (△); sum of minor products (□); charge passed (○); oxidation efficiency for the sum of epoxide and 2-hexanone (▽); oxidation efficiency of epoxyhexane (▲).

TABLE 1

Epoxidation of 2-Hexene on the Anode of Pt Black

Reactant	2,3-Epoxyhexane/mol · m^{-2}			C.P. (×10^4 C · m^{-2})	O.E. (epoxide) (%)
	cis-	*trans*-	Total		
cis-2-Hexene	0.634	0.004	0.638	70.7	17.4
trans-2-Hexene	0.001	0.340	0.341	70.7	9.3
cis-, *trans*-Mixture (1:1 mol/mol)	0.311	0.163	0.474	72.9	12.6

T = 303 K, reaction time 2 h, applied voltage 1.7 V, H_3PO_4 1.0 mol · dm^{-3}, 2-hexene 2 ml. Anode, Pt black, P(Ar) = 101 kPa. Cathode, Pt black/graphite, $P(H_2O)$ = 3 kPa, Ar balance.

different Pt black samples on the oxidation of 1-hexene under standard reaction conditions. The calcination of Pt blacks was performed in air at 673 K for 2 h. The pretreatment enhanced remarkably the catalytic activity of epoxidation for the Pt black sample we prepared and that obtained from Kanto. However, no effect was observed within the experimental error for the Pt black obtained from Wako.

The effects of calcination temperature for the Pt black (Kanto) on the results of 1-hexene oxidation are shown in Fig. 7. The pretreatment was done at a different temperatures for 2 h in air (101 kPa). The 1-hexene oxidation was performed under standard conditions. The results in Fig. 7 indicate that the calcination treatment of the Pt black at >423 K markedly improves the rate of oxidation of 1-hexene with a slight enhancement in the current or the charge passed. Therefore, the oxidation efficiencies for the formation of 1,2-epoxyhexane and the sum of 1,2-epoxyhexane and 2-hexanone are increased greatly at calcination temperatures >423 K. The results in Fig. 7 show that the optimum calcination temperature for oxidation of 1-hexene lies around 673 K. The treatment of the Pt black anode at a temperature higher than 700 K, however, decreased the electrocatalytic activity dramatically, probably due to a sintering of the sample. As described above, the Pt black sample obtained from Wako was quite active for oxidation of 1-hexene from the beginning in the absence of calcination pretreatment. The treatment did not influence the electrocatalytic activity in this sample. In contrast, the catalytic performance of the sample obtained from Kanto was improved by the treatment. In order to study the effect of the treatment on the oxidation state of the surface of both Pt black samples, we measured the XPS spectra of the samples.

e. XPS measurements. Figure 8 shows the Pt 4*f* XP spectra of the Pt black samples (Wako and Kanto) before and after the calcination treatment at 673 K for 2 h. The Pt 4*f* XP spectra of the sample were separated into 4 peaks. The separation curves are also shown in Fig. 8. The pair of peaks at 71.2 and 74.5 eV and the pair at 74.2 and 77.3

TABLE 2

Effect on the Epoxidation of 1-Hexene of Calcination of Pt Blacks

Anode	Products/mol · m^{-2}			C.P. (×10^4 C · m^{-2})	O.E. (%)		Select. (epoxide) (%)
	Epoxide	2-Hexanone	Others		Total	Epoxide	
Pt black (Wako)							
Without calcination	1.699	0.754	0.163	84.1	61.9	39.0	65.0
Calcined	1.758	0.804	0.195	88.4	62.7	38.4	63.8
Pt black (Kanto)							
Without calcination	0.035	0.003	0.015	45.6	2.5	1.5	65.9
Calcined	0.846	0.219	0.092	51.1	46.2	32.0	73.1
Pt black (prepared)							
Without calcination	0.126	0.036	0.042	77.7	5.8	3.1	61.8
Calcined	1.023	0.414	0.138	89.2	36.5	22.1	65.0

T = 303 K, reaction time 2 h, applied voltage 1.7 V, H_3PO_4 1.0 mol · dm^{-3}, 2-hexene 2 ml. Anode, Pt black, P(Ar) = 101 kPa. Cathode, Pt black/graphite, $P(H_2O)$ = 3 kPa, Ar balance.

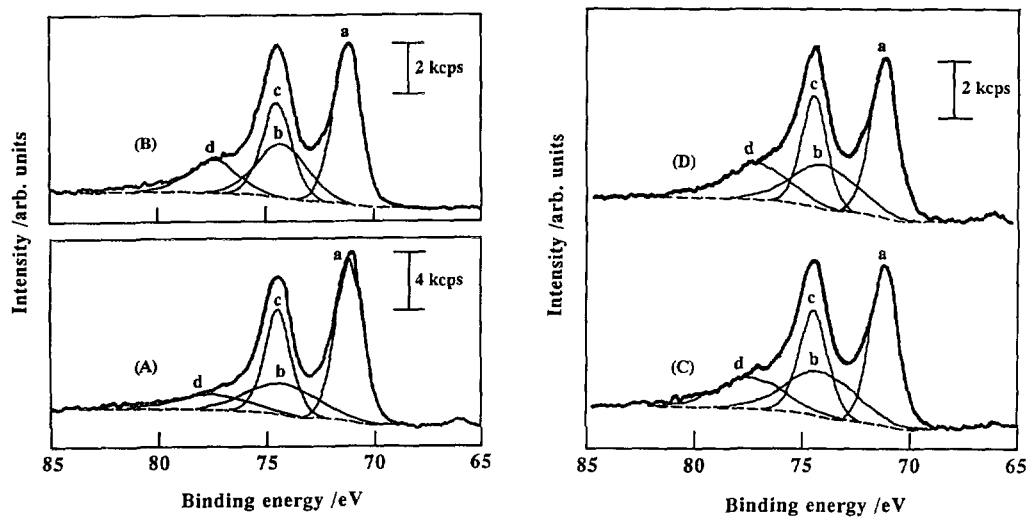

FIG. 8. Pt 4*f* X-ray photoelectron spectra of Kanto and Wako Pt black samples. (A) Kanto-non (Kanto-without calcination), (B) Kanto-clcn (Kanto-calcined), (C) Wako-non (Wako-without calcination), and (D) Wako-clcn (Wako-calcined). Peaks (a) and (c) represent Pt $4f_{7/2}$ and $4f_{5/2}$ levels of Pt^0, respectively. Peaks (b) and (d) represent Pt $4f_{7/2}$ and $4f_{5/2}$ levels of Pt^{4+}, respectively.

eV can be ascribed to platinum metal (Pt^0) and cation (Pt^{4+}), respectively (19–21, 25). As shown in Fig. 8, a contribution of the Pt^{4+} peaks to the Pt 4*f* XP spectra is significantly large for the three Pt blacks; Kanto-clcn (Kanto-calcined), Wako-non (Wako-without calcination), and Wako-clcn (Wako-calcined). For these thre Pt black samples, the peak ratio of Pt^{4+} to Pt^0 is found to be 0.65–0.72, suggesting that ca. 40% of the surface of these Pt blacks is a Pt^{4+} phase. On the other hand, the surface of Kanto-non (Kanto-without calcination) is composed of a comparable amount of Pt^0 and Pt^{4+} phases. The calcination of the Kanto Pt black leads to a considerable increase in the Pt^{4+} phase due to the oxidation of the Pt^0 phase. However, the Wako Pt black has a highly oxidized surface at the outset, and thus the Pt^{4+}/Pt^0 ratio at the surface has not been affected by the calcination. These observations strongly suggest that the electrocatalytic activity of Pt blacks for the oxidation of olefins is closely related to the formation of a Pt^{4+} phase at the surface.

The existence of a Pt^{2+} phase, possibly at 72.7 eV for $4f_{7/2}$ (21), on the surface of the Pt black samples can be excluded since the feature of the Pt 4*f* peak obtained in this study is quite different from that obtained for a mixture of the Pt^0 and Pt^{2+} phases ($Pt^0/Pt^{2+} = 1:1$) (21).

Figure 9 shows the O 1*s* XP spectra of the same Pt blacks shown in Fig. 8. For three samples (Kanto-clcn, Wako-non, and Wako-clcn), the O 1*s* XP spectrum was separated into 2 peaks (531 eV and 533 ~ 534 eV). The O 1*s* peak at 533 ~ 534 eV ($O_{(b)}$) was not appreciably observed on the Kanto-non sample. According to the literature (19, 21, 25), the O 1*s* peak at 531 eV ($O_{(a)}$) observed on an oxidized Pt surface is assigned to the O^{2-} anions binding to Pt^{4+} cations (oxygen of PtO_2 phase).

The O 1*s* peak at 533 ~ 534 eV ($O_{(b)}$) was detected for the Wako and Kanto-clcn Pt blacks but was not observed for the Kanto-non. This O 1*s* peak may be assigned to oxygen adsorbed on the surface Pt^{4+} cations. The FWHM (full width at half maximum) of this peak is unusually

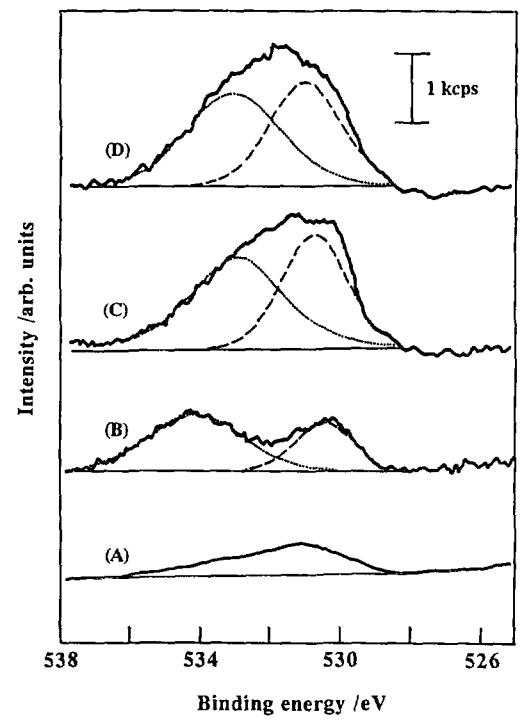

FIG. 9. O 1*s* XP spectra of various Pt blacks. (A) Kanto-non, (B) Kanto-clcn, (C) Wako-non, and (D) Wako-clcn. The separation curves are shown by dotted lines.

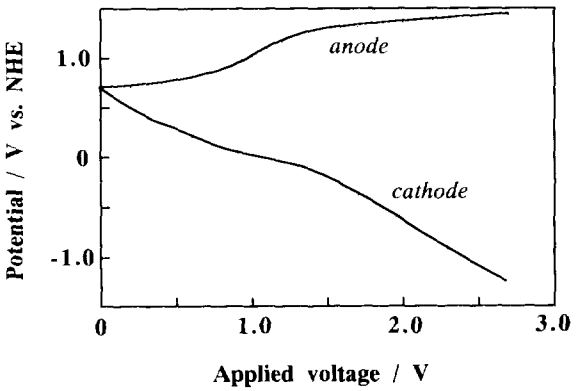

FIG. 10. The anode and cathode potential during oxidation of propylene as functions of applied voltage. The experiments were performed under standard conditions except for changing the applied voltage.

larger (3.2 ~ 3.3) than the reported FWHM (usually <2.3) for oxygen in the literature (21, 25). This suggests that the O 1*s* peak at 533 ~ 534 eV may be ascribed to at least two different oxygen species (26).

In any case, the XPS results described above indicate the presence of the PtO_2 phase at the surface and an oxygen species on Pt^{4+}. This oxygen species ($O_{(b)}$) is less negatively charged than the oxygen anion of PtO_2 ($O_{(a)}$). We suggest that this oxygen, $O_{(b)}$, might be steadily generated on the oxidized Pt blacks (PtO_2) under an applied voltage at >1.1 V, causing the epoxidation of propylene and other olefins.

f. Active sites and reaction mechanism. Before we discuss the active sites and reaction mechanism for the epoxidation of propylene, the anode potential during reaction should be investigated. Thus, the anode and the cathode potentials under standard reaction conditions were measured while changing the applied voltage across the cell during oxidation of propylene. The results are plotted as functions of the applied voltage in Fig. 10. Here, the applied voltage is the difference between the anode and the cathode potentials. Zero applied voltage means short-circuit conditions.

As described earlier, the oxidation of propylene was initiated at an applied voltage >1.1 V. According to the results in Fig. 10, this indicates that the reaction occurs at an anode potential greater than 1.1 V (vs NHE). Increase in the applied voltage from 1.0 to 1.5 V enhanced the formation rates of both propylene oxide and acetone remarkably (Fig. 2). A sharp increase in the anode potential was observed at this range of applied voltage (Fig. 10). Further increase in the applied voltage from 1.5 V increases the anode potential only slightly but decreases the cathode potential specifically, indicating an increase in the cathode overpotential for the reduction of H^+ into hydrogen (Eq. [2]). As can be seen from Fig. 2, the oxidation efficiency for the formation of oxygenates over this range of the applied voltage decreases sharply with the applied voltage, indicating an accelerated evolution of oxygen without oxidizing propylene.

It is to be recalled that the formation rates of propylene oxide and acetone were reduced with a rise in the applied voltage above 1.7 ~ 2.0 V. If the oxidation of propylene occurs according to a Langmuir–Hinshelwood-type mechanism between the adsorbed propylene and active oxygen on the surface of Pt black, the covering of the active sites with the active oxygen with a rise in the applied voltage must decrease the rates of formation of propylene oxide and acetone. We should consider another explanation for the decrease in the formation of propylene oxide and acetone at higher applied voltages >1.7 V, viz., a further oxidation of the formed propylene oxide and acetone into acetic acid and CO_2 which were in fact increased at >1.7 V. However, the decrease in the amount of propylene oxide and acetone at >2.0 V was not balanced with the increase in the amount of acetic acid and CO_2. Separate experiments for oxidations of propylene oxide and acetone as the starting substrate at an applied voltage of 2.2 V produced only CO_2 with a trace of acetic acid. Thus, the formation of acetic acid observed in Fig. 2 cannot be explained by the oxidation of the propylene oxide or of the acetone produced.

The standard redox potentials of platinum oxides in aqueous solution are shown below (27).

	Standard Potential vs NHE (V)
$PtO + 2H^+ + 2e^- = Pt + H_2O$	0.98
$PtO_2 + 2H^+ + 2e^- = PtO + H_2O$	1.05
$PtO_3 + 2H^+ + 2e^- = PtO_2 + H_2O$	2.00

According to these potentials, it should be noted that PtO_2 is thermodynamically the most stable phase under an applied voltage >1.1 V or an anode potential higher than 1.1 V vs NHE (see Fig. 10), which is required for the oxidation of propylene.

It is generally believed that the overall reaction pathway for oxygen evolution at the anode in acid electrolytes can be summarized as follows (28).

$$(H_2O)_{ads} \rightarrow (OH)_{ads} + H^+ + e^- \quad [A]$$

$$(OH)_{ads} + (OH)_{ads} \rightarrow (O)_{ads} + H_2O \quad [B]$$

$$\text{or } (OH)_{ads} \rightarrow (O)_{ads} + H^+ + e^- \quad [C]$$

$$(O)_{ads} + (O)_{ads} \rightarrow (O_2)_{ads} \quad [D]$$

$$(O_2)_{ads} \rightarrow O_2 \quad [E]$$

Here, the rate-determining step for oxygen evolution is

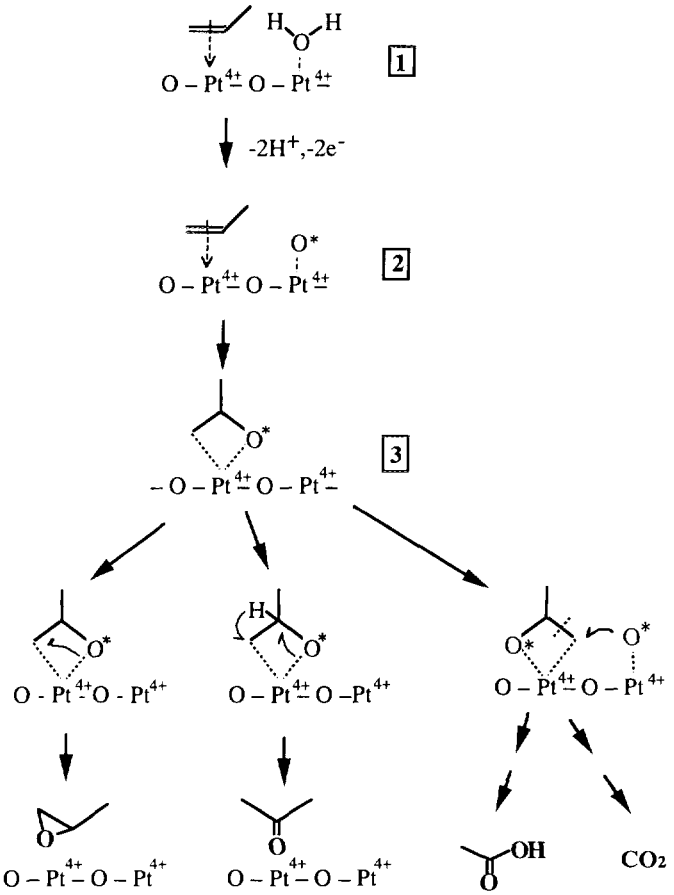

FIG. 11. Reaction mechanism for oxidation of propylene.

an electron-transfer step, the discharge of H_2O to form adsorbed OH radicals on the electrode surface (Eq. [A]). The subsequent fast reaction, either B or C, gives an adsorbed oxygen atom on the surface. The final step is oxygen evolution through reactions D and E. The number of other reaction pathways assuming various intermediates such as H_2O_2 and $(HO_2)_{ads}$ might be possible. However, at this moment, we have no direct evidence to identify the active oxygen species for epoxidation of olefins during electrolysis of water.

As described earlier, the possibility of H_2O_2 and $(HO_2)_{ads}$ as the reactive oxygen intermediate may be small. We can exclude OH radicals as well because neither hydroxylation of benzene nor partial oxidation of cyclohexane proceeded. It is well known that these reactions are caused by OH radicals under mild conditions (29–31). Therefore, we hypothesize that the nascent oxygen atoms generated through reaction [B] or [C] contribute to the oxidation of propylene on a PtO_2 surface at the anode. The tentative Langmuir–Hinshelwood-type reaction mechanism is demonstrated in Fig. 11. The active oxygen atom O* generated on Pt^{4+} adds to the π-orbital of propylene, forming a common reaction intermediate 3. Transformation of this intermediate gives propylene oxide and acetone in parallel. Further addition of oxygen to the intermediate 3 must result in the breaking of the C–C bond, giving CO_2 and acetic acid as the minor products probably through several additional steps.

As described above, the calcination of Pt black in air at 673 K enhanced the catalytic activity of the anode for 1-hexene oxidation. Pretreatment clearly increased the PtO_2/Pt ratio at the surface. This might change the morphology and the electronic state of the surface PtO_2 phase. These factors may strongly enhance the generation of O*, the adsorption of olefins, or the formation of intermediate 3. Further investigation is definitely needed to clarify these questions.

REFERENCES

1. Kirk, R. O., and Dempsey, T. J., *in* "Encyclopedia of Chemical Technology," Vol. 19, p. 246. Wiley, New York, 1982.
2. Goor, G., *in* "Catalytic Oxidations with Hydrogen Peroxide as Oxidant" (G. Strukul, Ed.), p. 13. Kluwer, Dordrecht, 1992.
3. Clerici, M. G., Bellussi, G., and Romano, U., *J. Catal.* **129,** 159 (1991).
4. Notari, B., *Stud. Surf. Sci. Catal.* **67,** 243 (1991).
5. Strukul, G., Zanardo, A., and Pinna, F., *Stud. Surf. Sci. Catal.* **55,** 81 (1990).
6. Tabushi, I., and Morimitsu, R., *J. Am. Chem. Soc.* **106,** 6871 (1984).
7. Tabushi, I., Kodera, M., and Yokoyama, M., *J. Am. Chem. Soc.* **107,** 4466 (1985).
8. Kuznetsonva, N. I., Lisitsyn, A. S., Boronin, A. I., and Likholobov, V. A., *Stud. Surf. Sci. Catal.* **55,** 89 (1990).
9. Sato, A., Miyake, T., Saito, T., *Shokubai (Catalyst)* **34,** 132 (1992).
10. Sakurai, H., Hataya, Y., Goromatsu, T., and Matsuura, H., *J. Mol. Catal.* **29,** 153 (1985).
11. Mansuy, D., Fontecave, M., and Bartoli, J. F., *J. Chem. Soc. Chem. Commun.*, 253 (1983).
12. Battioni, P., Bartoli, J. F., Ledue, P., Fontecave, M., and Mansuy, D., *J. Chem. Soc. Chem. Commun.*, 791 (1987).
13. Yamanaka, I., Nakagaki, K., Akimoto, T., and Otsuka, K., *Chem. Lett.*, 1717 (1994).
14. Mukaiyama, T., Takai, T., Yamada, T., and Rhode, O., *Chem. Lett.*, 1661 (1990).
15. Yamada, T., Takai, T., Rhode, O., and Mukaiyama, T., *Bull. Chem. Soc. Jpn.* **64,** 2109 (1991).
16. Mizuno, N., Hirose, T., and Iwamoto, M., *Stud. Surf. Sci. Catal.* **82,** 593 (1994).
17. Otsuka, K., Yoshinaka, M., and Yamanaka, I., *J. Chem. Soc. Chem. Commun.*, 611 (1993).
18. Yamanaka, I., and Otsuka, K., *J. Chem. Soc. Faraday Trans.* **81,** 1791 (1993).
19. Kim, K. S., Winograd, N., and Davis, R. E., *J. Am. Chem. Soc.* **17,** 6296 (1971).
20. Wagner, C. D., Riggs, W. M., Davis, L. E., and Moulder, J. F., *in* "Handbook of X-Ray Photoelecron Spectroscopy" (G. E. Muilenberg, Ed.), Perkin–Elmer Corp., MN, 1978.
21. Peuckert, M., Bonzel, H. P., *Surf. Sci.* **145,** 239 (1984).
22. Shirley, D. A., *Phys. Rev. B* **5,** 4709 (1972).
23. Sherwood, P. M. A., *in* "Practical Surface Analysis" (M. P. Seah and D. Briggs, Eds.), p. 573. Wiley, New York, 1990.

24. Otsuka, K., Yamanaka, I., and Hagiwara, M., *Chem. Lett.*, 1861 (1994).
25. Dickinson, T., Povay, A. F., and Sherwood, P. M. A., *J. Chem. Soc. Faraday Trans. I* **71,** 298 (1975).
26. Paál, Z., and Schlögl, R., *Surf. Interfac. Anal.* **19,** 524 (1992).
27. Pourbaix, M., "Atlas d'Equilibres Electrochimiques à 25°C," p. 300. Gauthier Villars, Paris, 1963.
28. Kinoshita, K., "Electrochemical Oxygen Technology," p. 89. Wiley, New York, 1992.
29. Haber, F., and Weiss, J., *Proc. Roy. Soc. (London)* **A147,** 332 (1934).
30. Walling, C., and Johnson, R. A., *J. Am. Chem. Soc.* **97,** 363 (1975); Walling, C., *Acc. Chem. Res.* **8,** 125 (1975).
31. Matsue, T., Fujihira, M., and Osa, T., *J. Electrochem. Soc.* **128,** 2565 (1981).